Chinese Journal of
POLYMER SCIENCE

REVIEW

https://doi.org/10.1007/s10118-022-2878-y
Chinese J. Polym. Sci. **2023**, *41*, 500–515

Interfacial Engineering of Polymer Blend with Janus Particle as Compatibilizer

Hai-Ling He and Fu-Xin Liang*

Institute of Polymer Science and Engineering, Department of Chemical Engineering, Tsinghua University, Beijing 100084, China

Abstract Mixing two or more polymers to produce the "polymer alloy" is one of the most versatile and economical strategies for developing new polymeric materials. The compatibility between polymer components largely determines the comprehensive performance of polymer blend. More recently, a type of unique surface partitioned materials, Janus particles, has been proposed to act as a novel interfacial compatibilizer for polymer blends. Such Janus particles integrates the amphipathicity of diblock copolymer and interfacial stabilization of nanoparticles, displaying a significant superiority in comparison with molecular compatibilizers for a wide range of polymer blends. In this review, we mainly focus on the compatibilizing effects of Janus nanofillers of various morphologies, including spherical, snowman-like, and two-dimensional nanosheets, on polymer blends. We shed light on the impacts of compatibilization of Janus particles on phase morphologies, mechanical properties, and functionalities of polymer blends. This review could provide a guidance for designing an effective Janus particle compatibilizer to develop high-performance polymer blends.

Keywords Janus particles; Compatibilizer; Polymer blend; Interfacial engineering

Citation: He, H. L.; Liang, F. X. Interfacial engineering of polymer blend with Janus particle as compatibilizer. *Chinese J. Polym. Sci.* **2023**, *41*, 500–515.

INTRODUCTION

Polymeric materials have gained a wide and sustained attention attributing to their excellent properties since being invented. However, with the growing demand for high-performance, multifunction, and intellectualization of polymers, one-component polymer is increasingly unable to meet its application in many fields. The blending technology that physically mixing two or more polymers forms macroscopically uniform and stable "polymer alloy" is the most versatile and economical strategy for developing desirable polymeric materials. Nevertheless, because most polymer pairs are thermodynamically immiscible, simply mixing two or more polymers generates the phase separation, which generally leads to some large size of discrete domains distributed in the continuous matrix and forming a poor interface between polymer components.[1,2] Such blends with a phase separated structure cannot play individual advantages of each polymer component, hence, the mechanical and functional properties of blends are not improved as expected, restricting the development of high-performance polymeric blends.

Introducing compatibilizer into the immiscible blend system is regard as an efficient strategy to tailor the phase morphology and enhance the interface adhesion of polymer blends.[3,4] Some common compatibilizers, *e.g.*, amphiphilic diblock copolymers, micro- and nanofillers, have been used to compatibilize various immiscible blends.[5–7] However, these conventional compatibilizers cannot simultaneously realize the easy migration to the interface and steadily anchoring at the interface of polymer components, particularly not integrating the effects of both compatibilization and functionalization. Recently, Janus particles (JPs) have been proposed to act as a novel compatibilizer to regulate phase morphology and interfacial properties of polymer blends. Janus particles are one type of surface partitioned materials, which possess different chemical compositions or physical properties on two sides of the same particle.[8,9] Such Janus particles with unique microstructure combine the advantages of both amphipathic diblock copolymers and nanoparticles, which could not only readily migrate to the interface due to selectively interacting with two polymer components, but also stabilize at the interface.[10] Janus particles, the desirable compatibilizer, can synchronously refine the size of dispersed phases and customize the interfacial properties, endowing the blends with excellent mechanical properties and functionality.[11–13]

This work reviews the state of the art of Janus particles for compatibilization of polymer blends. Firstly, some basic concepts of polymers blending and phase morphology of blend are briefly given. Then, the compatibilization of some traditional reactive and non-reactive compatibilizers for polymer

* Corresponding author, E-mail: liangfuxin@tsinghua.edu.cn

Special Issue: The Youth Innovation Promotion Association of the Chinese Academy of Sciences
Received August 9, 2022; Accepted October 10, 2022; Published online December 28, 2022

blends are overviewed. Emphasis is placed upon the compatibilizing effects of the Janus particles with diverse microstructures, *e.g.*, spherical, snowman-like and nanosheets, for polymer blends, including their impacts on phase morphologies, mechanical properties and functionalities of blends. In addition, the main synthesis method of Janus particles of various shapes acted as compatibilizers are outlined as well. Finally, an outlook on the further development and application of this polymer blend system introduced by Janus particles is given at the end of this review.

MISCIBILITY AND PHASE MORPHOLOGY OF POLYMER BLEND

The compatibility of two or more polymers plays a vital role on properties of polymer blend. In a blend system, the thermodynamic compatibility of polymer refers to the ability of polymers to dissolve into each other and form homogeneous systems, which can be predicted by the Gibbs free energy of mixing, ΔG_{mix}. To realize the miscibility of polymer blend, the following inequality must be met:[14]

$$\Delta G_{mix} = \Delta H_{mix} - T\Delta S_{mix} < 0 \quad (1)$$

$$\left[\frac{\partial^2 \Delta G_{mix}}{\partial \phi_i^2}\right]_{T,P} > 0 \quad (2)$$

where ΔH_{mix}, ΔS_{mix} are enthalpy and entropy of mixing, respectively, ϕ_i is the volume fraction of component, T and P represent the fixed temperature and pressure, respectively. Generally, the entropy of mixing for polymer blend ΔS_{mix} is very low due to the nonexistence of strong intermolecular interaction and chemical bonds breaking and recombination in blend system. And because the mixing of polymers is an endothermic process, the enthalpy of mixing ΔH_{mix} is positive value. Thus, for most of polymer blends, there are $\Delta G_{mix} > 0$, forming a completely immiscible blend (Fig. 1A, curve a). Only if the entropic contribution is more than the enthalpic contribution, which exists a remarkable intermolecular interaction between blend components, a negative ΔG_{mix} could be realized, thus obtaining a completely miscible or partially miscible blend (Fig. 1A, curves b and c).[15,16]

The miscibility of blend, including miscible, compatible, and immiscible blends, determines their phase morphologies. Completely miscible blends have homogeneous morphologies on nanoscale due to strong interactions, however, they are limited to certain polymer blends, *e.g.*, polystyrene/poly(phenylene oxide) (PS/PPO).[17] Partially miscible blends are also referred to as compatible blends, in which part of one polymer can be dissolved in the other polymer, exhibiting a fine-phase morphology, for example the polycarbonate /poly(acrylonitrile-butadiene-styrene) (PC/ABS) blend.[18] A majority of polymer blends are immiscible arising from the negligible entropy of mixing, ΔS_{mix}, *e.g.*, polypropylene (PP)/PS, poly(ethylene terephthalate)/poly(vinyl alcohol) (PET/PVA) blends. The immiscibility of blend components normally causes the phase separation during blending, resulting in the formation of various phase morphologies with a weak interface. The morphologies of immiscible blends can be summed up as dispersed structure and co-continuous structure, among which dispersed structure includes sea-island (droplet morphology or domain morphology, Fig. 1B), laminar (Fig. 1C), fiber (Fig. 1D), and double emulsion (Fig. 1E).[19,20] The sea-island morphology is the most common microstructure in immiscible blends, in which the low-content polymer component forms a dispersed phase, presenting an 'island' distribution, and the high-content polymer component forms a continuous phase, displaying a 'sea' distribution. Furthermore, this typical sea-island morphology can produce the fiber or laminar structure under melt shear stretching. Co-continuous (or bicontinuous) structure (Fig. 1F) is termed as an interpenetrating polymer blend with a dual-phase continuity or co-phase continuity, in which at least a part of each polymer component can form a coherent structure throughout the whole blend.[21,22] The blend with co-continuous morphology possesses a superior performance than the blend with dispersed morphology in many aspects since it can maximize the individual properties of each polymer component.[23] However, in general, the co-continuous morphology only forms within a certain range of volume fractions of polymer component (*e.g.*, near phase inversion point), which is related to the viscosities of polymer components.[24,25]

The phase morphologies of blends can significantly influence their performance. For example, reducing the domain size of dispersed structure or constructing the co-continuous structure in blends can improve their mechanical strength and toughness, and conductive functionality. The morpholo-

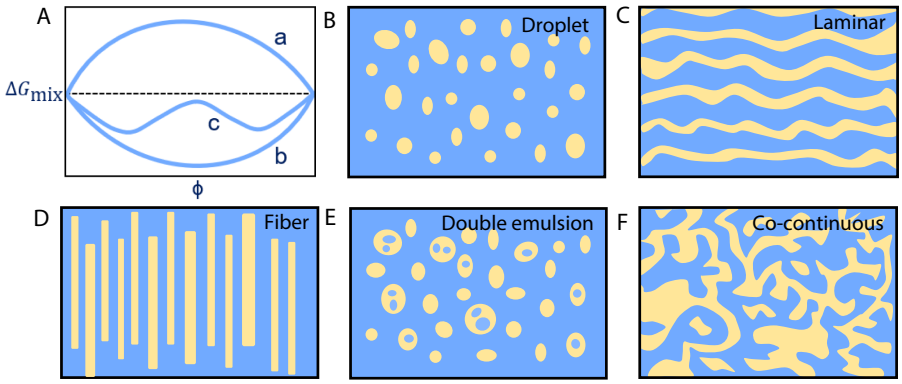

Fig. 1 (A) Variations of Gibbs free energy of mixing (ΔG_{mix}) with volume fraction of component, ϕ, curves a, b, and c represent completely immiscible, completely miscible, and partially miscible, respectively.[15,16] Morphologies of immiscible polymer blends,[19,20] (B) droplet, (C) laminar, (D) fiber, (E) double emulsion, (F) co-continuous.

https://doi.org/10.1007/s10118-022-2878-y

gies of blend mainly depend on volume or weight ratio, interfacial tension (compatibility), and viscosity ratio of polymer components, and processing condition. In general, due to the determined components and proportions, and limited adjust for processing condition, improving the compatibility between polymer components (namely compatibilization) is an effective strategy for tailoring the phase morphologies of blends, meanwhile compatibilization effect could enhance the interfacial adhesion of polymers as well.

COMPATIBILIZATION OF POLYMER BLEND

Improving the compatibility between polymer components of blend system by compatibilization effect mainly lies in reducing the interfacial tension between polymers, thus facilitating a large interfacial contact area and strong interfacial adhesion.[26,27] With respect to thermodynamic principle (Eq. 1), the enthalpy of mixing $\Delta H_{mix} < 0$ is required for compatibilizing of blend ($\Delta G_{mix} < 0$) due to negligible entropy of mixing ($\Delta S_{mix} \approx 0$). The reduction of interfacial tension or $\Delta H_{mix} < 0$ could be achieved by enhancing the intermolecular interaction of polymer components, *e.g.*, introducing strong covalent bonds, ionic bonds, or weak intermolecular forces. The addition of compatibilizer in blend is the most common way to improve the intermolecular interaction, and further realizing the compatibilization of blend. The commonly used compatibilizers, including block or graft copolymers, low or high molecular reactive compatibilizers, and micro- or nano-fillers,[28,29] possess good compatibility with two polymer components of blend. Since these compatibilizer molecules contain some groups that can physically or chemically bind to the molecular chains of two polymers, respectively.

Non-reactive compatibilizer is usually block or graft copolymer consisted of two or more blocks (Fig. 2A).[30] It is analogous to a surfactant, the block a of copolymer has a strong affinity with polymer a of blend system, and the block b of copolymer can interact with polymer b. Reactive compatibilizer contains an active functional group, which can generate chemical bonding with molecular chains of polymer component. For instance, some low molecular reactive compatibilizers include isocyanate chain extenders containing —NCO groups, *e.g.*, methylene-diphenyl diisocyanate (MDI), toluene diisocyanate (TDI), lysine triisocyanate (LTI) and polyphenyl polymethylene polyisocyanate (PAPI), free radical initiators, *e.g.*, dibenzoyl peroxide (BPO), dicumyl peroxide (DCP), triphenyl phosphite (TPP), and epoxy chain extenders, which could chemically react with end groups of polymer component.[31] In addition, some high molecular polymers with active groups are also applied as reactive compatibilizers for polymer blend due to reactive formation of graft or lightly cross-linked copolymer (Fig. 2B).[30]

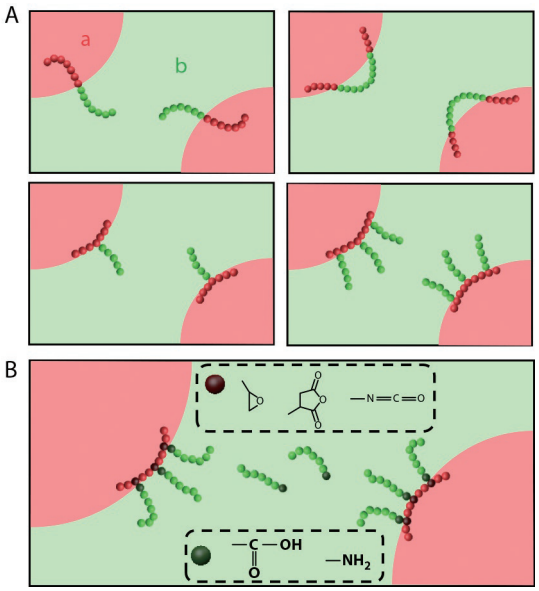

Fig. 2 Schematic diagram of interfacial distribution of various compatibilizers in polymer blend,[30] (A) diblock, triblock, single-graft copolymer, and multiple-graft copolymer, (B) compatibilization mechanism of partial reactive compatibilizers.

The micro- or nano-fillers not only possess Pickering effect of stably locating at interface, but also are capable to integrate multifunction. Hence, the micro- and nano-fillers with different microstructures, *e.g.*, zero-dimensional polyhedral oligomeric silsesquioxane (POSS) and quantum dots, one-dimensional carbon nanotubes (CNTs) and nanofibers with large aspect ratio, two-dimensional graphene, montmorillonite (MMT) and clay, and three-dimensional silica, metal-oxide nanoparticles, are also used as compatibilizers for polymer blend.[32–36] The compatibilization of nanofillers are related to their location in blend. Generally, the nanofillers preferentially localize in the polymer that has a strong affinity with nanofillers. Only when the nanofillers have a similar affinity with two polymer components, they can selectively localize at the interface of polymers. The distribution of nanofillers in blend can be predicted by a wetting coefficient ω, according to Young's equation:[37]

$$\omega = \frac{\gamma_{N\text{-}B} - \gamma_{N\text{-}A}}{\gamma_{A\text{-}B}} \quad (3)$$

where $\gamma_{N\text{-}A}$, $\gamma_{N\text{-}B}$, $\gamma_{A\text{-}B}$ are the interfacial tension between nanofillers and polymer A, nanofillers and polymer B, polymer A and B, respectively. When $\omega > 1$ or $\omega < -1$, the nanofillers distribute in polymer A or B, respectively. And if $-1 < \omega < 1$, the nanofillers could locate at the interface between polymer A and B. In practice, except for wetting coefficient, the microstructure of nanofiller, viscosity ratio of polymer components, processing condition (*e.g.*, mixing procedure, blending time, *etc.*) also influence the distribution location of nanofillers in blend. This indicates the selective localization of nanofillers in blend depends on many factors.

COMPATIBILIZATION OF JANUS PARTICLES FOR POLYMER BLEND

Compatibilizers could generate the physical or chemical interactions with polymer components, further reducing the interfacial tension between two polymer components, thus improving the compatibility of polymers. However, the copolymers used as compatibilizers must have appropriate molecular weights. Copolymers with low molecular weights possess a weak interpenetration and entanglement with polymer components, thus readily desorbing form the interface, while the copolymers with high molecular weights are no picnic to migrate to the interface. Besides, copolymers are easy to

aggregate and thus form micelles distributing in the polymer domains.[38] And copolymer compatibilizers is prone to being destructed and losing under high-speed shear process.[39] Another homogeneous nanofiller compatibilizers can increase the viscosity of blend, further impeding coalescence of polymer domains, and thus refining the domain size. But the nanofillers are hard to enhance the interfacial adhesion due to the harsh terms for nanofillers migrating to the interface.[40] Therefore, a novel compatibilizer need to be developed to improve the compatibility of immiscible polymers. Janus particles (JPs) integrate the selective interaction abilities of block copolymers (easily migrating to the interface) with interfacial stabilization of nanoparticles, presenting a promising potential to act as efficient compatibilizers of immiscible blends.[41,42]

Synthesis of Janus Particle Compatibilizers with Different Morphologies

Various Janus nanoparticles with anisotropic shapes, such as sphere, snowman-like, two-dimensional nanosheets, *etc*., have been synthesized for compatibilizing usage (Fig. 3A).[43]

Spherical Janus nanoparticles

In earlier research, Janus micelles have been synthesized based on the amphiphilic nature of block copolymers consisted of incompatible blocks and their solution behavior.[44] In a selective solvent, the binary or ternary block copolymers could self-assemble or dissolve on a molecular level, where their less soluble blocks form core, and meanwhile the core is surrounded by a highly swollen corona of the more soluble blocks.[45–48] For example, Erhardt *et al*. synthesized the amphiphilic surface-compartmentalized nanoparticles through the above method based on linear ABC triblock copolymers (polystyrene-block-polybutadiene-block-poly(methyl methacrylate) (SBM)) (polybutadiene (PB), poly(methyl methacrylate) (PMMA)).[44] As shown in Fig. 3(B), the SBM film with lamellae of outer PS and PMMA blocks embedding spherical domains of PB middle blocks is firstly obtained by solution casting. Subsequently, the selectively cross-linking of spherical domains of PB middle blocks are carried out in a well-ordered bulk. Then the redissolution of bulk phase in a good solvent realizes the compartmentalization of the outer PS and PMMA blocks, and further formation of two hemisphere due to the microphase-segregation.

Snowman-like Janus nanoparticle

As our group reported previously,[49] the polymer@silica snowman-like Janus nanoparticles (JNPs) can be prepared by seed emulsion polymerization. Taking the aqueous dispersion of polymeric particles (*e.g*., PS/poly(divinylbenzene) (PDVB)) as seed emulsion, a 3-methacryloxypropyltrimethoxysilane (MPS) monomer-in-water emulsion containing surfactant sodium dodecyl sulfate (SDS) and initiator potassium peroxodisulfate (KPS) is formed at ambient temperature and dropped into seed emulsion to swell the polymer seed. Then, under stirring at 70 °C, the free radical polymerization of MPS is carried out to form a polyMPS (PMPS), and subsequently the sol-gel process of PMPS is gradually progressed. As the reaction proceeds, the generated PMPS polymer (organo-silica) forms a bulb on seed surface due to the phase separation between polymer seed and PMPS, thus snowman-like polymer@silica Janus nanoparticles can be attained (Fig. 3C). Moreover, the snowman-like JNPs with silica lobes of varied sizes can be obtained as well by adjusting the mass ratios of silicon monomer (MPS) and PS/PDVB polymer seed (SEM images in Fig. 3C). Besides snowman-like JNPs, the triblock JNPs with two silica lobes were also prepared by two-step seed emulsion polymerization (Fig. 3D).[50] Both polymer side and silica lobe of JNPs are reactive, which can be specifically modified to graft the active groups or polymer chains for preferable compatibilization.

Janus nanosheets

The Janus nanosheets as solid surfactants could preferably stabilize the interface of polymer blend due to their irregular shapes and large aspect ratios. Liang *et al*. developed a facile approach for large-scale preparation of amphiphilic Janus nanosheets through crushing Janus hollow spheres (as presented in diagram of Fig. 3E),[51] in which this Janus hollow sphere is prepared by a self-assembled so-gel process at an amphiphilic emulsion interface to generate a shell. For instance, under acidic condition, the sol-gel process preferentially proceeds at the interface, the hydrophilic species face aqueous phase outward the emulsion droplets, while the hydrophobic species face the oil phase inside the emulsion droplets. As a sol-gel process proceeds, the silicious materials cross-link at the interface, and further forming hollow sphere. The as-prepared hollow spheres are crushed into Janus nanosheets using colloid milling (SEM images of Fig. 3E). In addition, other oil soluble monomers and initiator can also be added to the interior oil phase, and the polymerization of monomers induces phase separation, subsequently aggregates of polymer forming a polymer layer on the lipophilic side (Fig. 3F).[52] Hence, a polymer-inorganic layered Janus nanosheets could be obtained by crushing the prepared Janus composite hollow spheres (SEM images of Fig. 3F). Furthermore, being ascribed to the active groups on surface of Janus nanosheets, some functional nanoparticles can be selectively conjugated onto one side of Janus nanosheets.

In addition, Janus particles with other architectures, such as one-dimensional Janus nanorods (or Janus cylinders, nanotubes, nanofibers) have been synthesized as well. Müller *et al*. fabricated the SBM Janus cylinders using the same method displayed in Fig. 3(B) only by increasing the weight fraction of the inner PB block, while keeping the weight fractions of the outer blocks (PS and PMMA) symmetric (Fig. 3G, i).[53] Brush block copolymers could also form the one-dimensional Janus microstructure by the self-assembly (Fig. 3G, ii).[54] The attachment of two or more types of side chains to a polymer backbone to form this brush copolymer, in which the side chains are long enough to drive segregation, and behave like "s" block segment. Then the as-received brush copolymer can self-assemble into nanometer-scale Janus microstructure. Moreover, the as-prepared one-dimensional nanorods (*i.e*., boehmite nanorods), carbon nanotubes (CNTs), nanofibers, *etc*. could also be modified to the Janus materials by the "*in situ*" reaction during melt blending. For example, Li *et al*. grafted the both PMMA tails and epoxide groups onto the boehmite nanorods and CNTs, and further producing the poly($_L$-lactic acid)/poly(vinylidene fluoride) (PLLA/PVDF) Janus nanorods and nanotubes when they were applied to compatibilize the immiscible PLLA/PVDF blends (Fig. 3G, iii).[55–57] And these one-dimensional Janus materials located at the interface of blends perform an excellent compatibilization, improving the mechanical properties and functionalities (*i.e*., electrical conductivity and flame retardancy).

https://doi.org/10.1007/s10118-022-2878-y

Compatibilization of Typical Janus Particles for Polymer Blend

Regarding Janus particles as compatibilizer for polymer blend, the microstructure characteristic of Janus particles, *e.g.*, shape, surface area, size and aspect ratio, are of great importance to phase morphology regulation and morphology stabilization of immiscible blends. For example, in comparison to the Janus particles with low aspect ratio, the high aspect ratio of Janus fillers could more effectively decrease the domain size of discreate phases at a low additive amount.

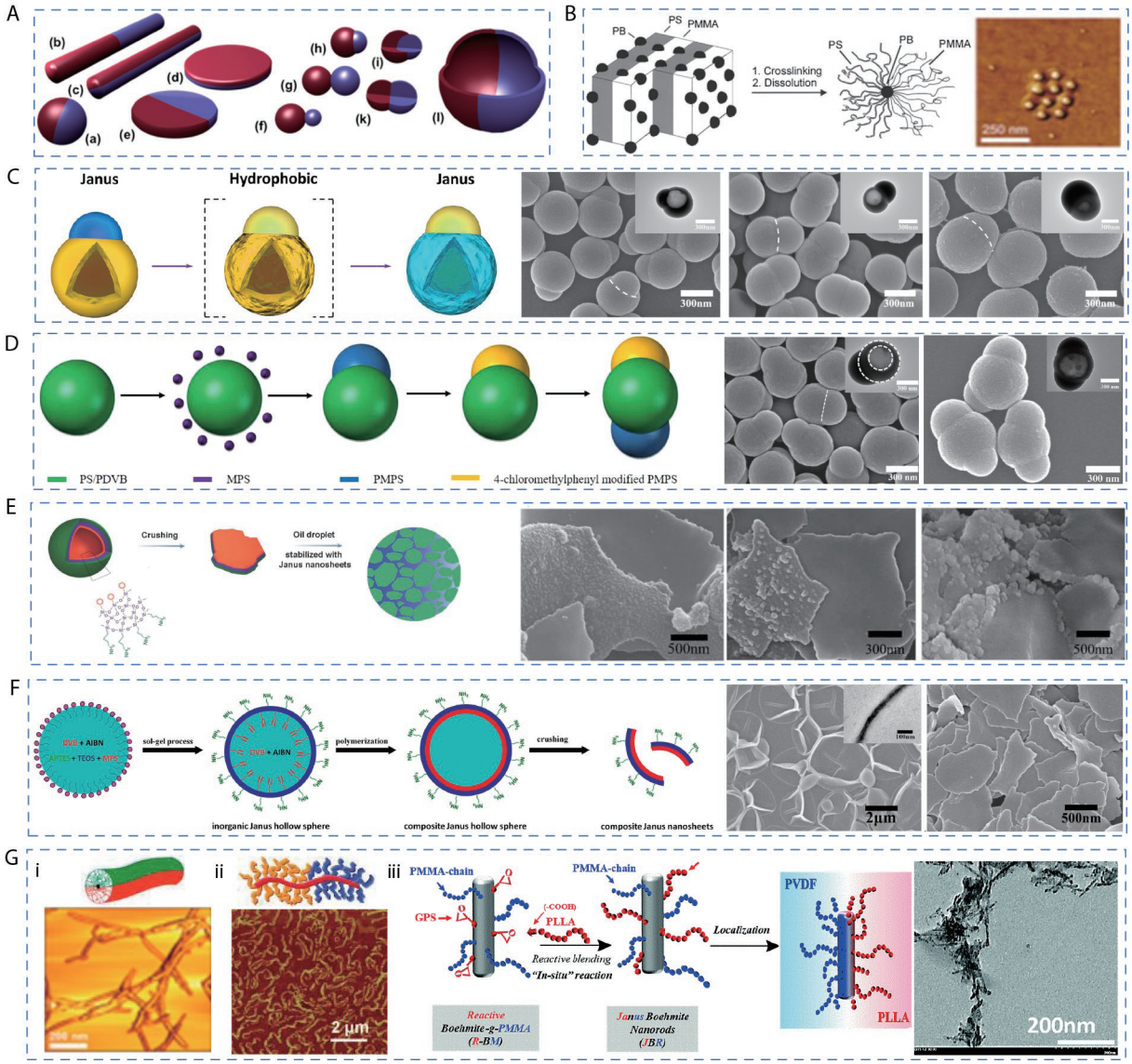

Fig. 3 (A) Different shapes of Janus particles (JPs) (a: spherical, b, c: cylindrical, d, e: disc-shaped, f–k: various dumbbell-shaped JPs, l: Janus vesicles or capsules). (Reprinted with permission from Ref. [43], Copyright (2013) American Chemical Society). (B) Schematic of synthesis and scanning force microscopy (SFM) images of SBM Janus micelle. (Reprinted with permission from Ref. [44], Copyright (2001) American Chemical Society). (C) Diagram of snowman-like Janus particles. Scanning electron microscopy (SEM) and inset transmission electron microscopy (TEM) images of snowman-like PS/PDVB@Silica Janus particles with varied size ratios of silica side and PS/PDVB side. (Reprinted with permission from Ref. [49], Copyright (2015) American Chemical Society). (D) Schematic of synthesis and SEM, inset TEM images of diblock and triblock Janus particles. (Reprinted with permission from Ref. [50], Copyright (2019) American Chemical Society). (E) Schematic fabrication of Janus nanosheets and acting as a solid surfactant. SEM images of Janus nanosheets labeled with sulfonated PS nanoparticles, amine-capped SiO_2 and trisodium citrate capped Fe_3O_4 nanoparticles. (Reprinted with permission from Ref. [51], Copyright (2011) John Wiley and Sons). (F) Schematic synthesis of polymer-inorganic Janus nanosheets. SEM and cross-section TEM image of Janus composite hollow sphere and corresponding Janus nanosheets. (Reprinted with permission from Ref. [52], Copyright (2012) American Chemical Society). (G) (i) Schematic diagram and morphology of SBM Janus cylinders, (Reprinted with permission from Ref. [53], Copyright (2003) American Chemical Society). (ii) AFM phase images of Janus cylindrical block brushes, (Reprinted with permission from Ref. [54], Copyright (2009) American Chemical Society). (iii) Fabrication schematic of PMMA/PLLA Janus nanorods by "*in-situ*" reaction, TEM images of boehmite nanorods with PMMA tails and epoxide groups. (Reprinted with permission from Ref. [56], Copyright (2019) The Royal Society of Chemistry).

Compatibilization of spherical Janus nanoparticles

Spherical Janus particles (JPs) that the tightly crosslinked polymer and the compatible polymer chains with blends are used as core and two hemispherical brushes, respectively, are firstly applied to compatibilize the immiscible blend. For example, Müller *et al*. prepared the spherical SBM Janus nanoparticles (JNPs) consisted of a tightly crosslinked PB nanoparticle core (8–10 nm) and two PS/PMMA hemispheres to compatibilize the PS/PMMA blend (Fig. 4A).[42] Owing to the higher adsorption energy at the interface of JNPs than that of block polymer, almost all of SBM JNPs could strongly adsorb and orient at the interface even under the high temperature and shear conditions, thus decreasing the PMMA domain diameter from 1.1 μm (PS/PMMA, 8/2) to 80 nm for 20 wt% JNPs content, achieving this nano-structuring of polymer blend. It is also found that the compatibilization efficiency of JNPs is superior to that of SBM ternary block copolymer (Fig. 4B). In addition, the same SBM JNPs were added to the PS/PMMA solution system to trap the changes of blend morphology induced by the variation of PS/PMMA mixing ratio and JNPs loading during solvent evaporation.[58] The JNPs can also stabilize the bicontinuous morphologies in cast film above glass transition temperature through assembling into a densely packed monolayer at the interface, which is able to inhibit coarsening and coalescence of phase-separated domains (Fig. 4C). Moreover, except for the PS/PMMA blend, the SBM JNPs can be also extended to compatibilize the technologically relevant polymer blend, *e.g.*, poly(2,6-dimethyl-1,4-phenylene ether) (PPE) and poly(styrene-*co*-acrylonitrile) (SAN), and the compatibilization process is proceeded at an industry-scale (Fig. 4D).[59] The compatibilizer of SBM JNPs could not only decrease the diameter of discrete droplets, but also alter the phase morphologies of blend, from elongated, irregular droplets, resembling a co-continuous phase for neat blend (Fig. 4E, i), turning into the morphology of small PPE droplets (dark) embedding in a continuous SAN matrix (Fig. 4E, ii). Due to the stabilization of JNPs at the interface reducing the interfacial energy, and thus repulsing the droplets coagulation, the diameters of most PPE domains are less than 1 μm, and far below the PPE sizes of neat blend and the blend filled with SBM triblock terpolymer (Fig. 4E, ii and iv). Moreover, a double emulsion morphology of the larger PPE droplet engulfing smaller SAN droplets was observed as well (Fig. 4E, iii), in which the JNPs densely anchor at all interface (black dots). The outstanding compatibilizing effect of SBM spherical Janus particles could be attributed to that they are prone to anchor at the blend interface, stemming from their nano-scale size and matrix-compatible polymer chains on two hemispheres. In the early stage of research, it was difficult to realize the large-scale production of Janus nanoparticles by self-assembly of block copolymer, which greatly limited the industry-scale research. Therefore, most researches focused on the control of the size and morphology of the phase region, while the mechanical properties are rarely studied.

In addition to directly introducing the JNPs into blend, the Janus particles formed during melt blending process can also realize an *in situ* reactive compatibilization of immiscible blends. Li *et al*. grafted the epoxy groups and PMMA chains onto the SiO_2 nanoparticles. When the modified nanoparticles were incorporated into a melt mixing PLLA/PVDF blend, the PLLA chains were further *in situ* grafted on the SiO_2 due to the reaction of COOH groups of PLLA with epoxide groups on the surface of SiO_2, thus forming the Janus nanoparticles (JNPs) with PLLA and PMMA chains (Fig. 4F, i).[60] The *in situ* formed PLLA/PMMA Janus SiO_2 nanoparticles play a significant compatibilizing effect to suppress coalescence of PVDF domains and increase the interfacial adhesion (Fig. 4F, ii and iii). Furthermore, the reactive compatibilizer of Janus nanomicelles (JNMs) can be also prepared using the same technology of *in situ* reactive melt blending (Fig. 4G).[61,62] Li *et al*. synthesized a poly(styrene-*co*-glycidyl methacrylate)-graft-poly(methyl methacrylate) (P((S-*co*-GMA)-*g*-MMA)) copolymer (reactive graft copolymer, RGC) *via* the "grafting-through" strategy. This copolymer incorporated into the PLLA/PVDF blend could form the Janus nanomicelles with PLLA and PMMA as hemispheres and PS as core at the interface. These JNMs located at the interface of PLLA/PVDF act as an effective compatibilizer to improve greatly the ductility of blend by an interfacial micelle compatibilization (IMC) mechanism. Besides, they also used caged polyhedral oligomeric-silsesquioxane (POSS) as a core to prepare the Janus nanoparticle.[63] They found that the compatibilizing effects of nanoparticles was closely related to the processing strategy. The PLLA-premixed sequence (first grafting PLLA onto the POSS core) played the best compatibilization for the PLLA/PVDF blend due to more POSS Janus nanoparticles being located at the PLLA/PVDF interface (Fig. 4H).

Compatibilization of snowman-like Janus nanoparticles

The snowman-like Janus nanoparticles (S-JNPs), whose self-structure consists of two hemispheres, can be selectively modified for compatibilizing various polymer blends. He *et al*. prepared a SiO_2@PDVB S-JNPs, and modified two hemispheres by grafting polyisoprene (PI) and polybutadiene (PBd) chains, respectively.[64] The obtained PI-J-PBd was applied to compatibilize PI/PBd blend, and trapped bicontinuous phase morphology in the rubber blend (Fig. 5A, i). Neat PI/PBd blend displays a sea-island phase structure with large PBd domains (Fig. 5A, ii). With introduction of PI-J-PBd into blend, average size of the PBd domains is generally decreased, and achieve a bicontinuous structure at 5.5 wt% PI-J-PBd (Fig. 5A, iii–vii). For the compatibilization of liquid isoprene rubber (LIR) and epoxy resin (ER) blend, Chen *et al*. grafted the dodecyl mercaptan (DM) and 3-(trimethoxysilyl) propyl methacrylate (MPS) chains onto PDVB and SiO_2 lobes of SiO_2@PDVB S-JNPs, respectively.[65] The MPS-SiO_2@PDVB-DM S-JNPs embedded in the interface of LIR and ER improve their compatibility. As the dosages of S-JNPs increase, the LIR domain sizes generally reduce from 6–24 μm for LIR/EP to 3–9 μm for LIR/EP/7% S-JNPs, and domain sizes become more uniform (Fig. 5B, i–vi). Moreover, Chen *et al*. compared the effects of homogeneous nanoparticles (SiO_2, SiO_2-TETA) and snowman-like Janus particles (TETA-SiO_2@PDVB) on phase domain sizes for acrylic resin/epoxy resin (AR/EP) blend (triethylenetetramine, TETA) (Fig. 5C), in which the TETA-SiO_2@PDVB S-JNPs anchored at the interface of AR/ER improve the compatibility of blend, significantly decreasing the dispersed phase sizes.[66] Besides, the polystyrene/silica (PS/SiO_2) S-JNPs were synthesized by a miniemulsion polymerization technique and applied to compatibilize the

https://doi.org/10.1007/s10118-022-2878-y

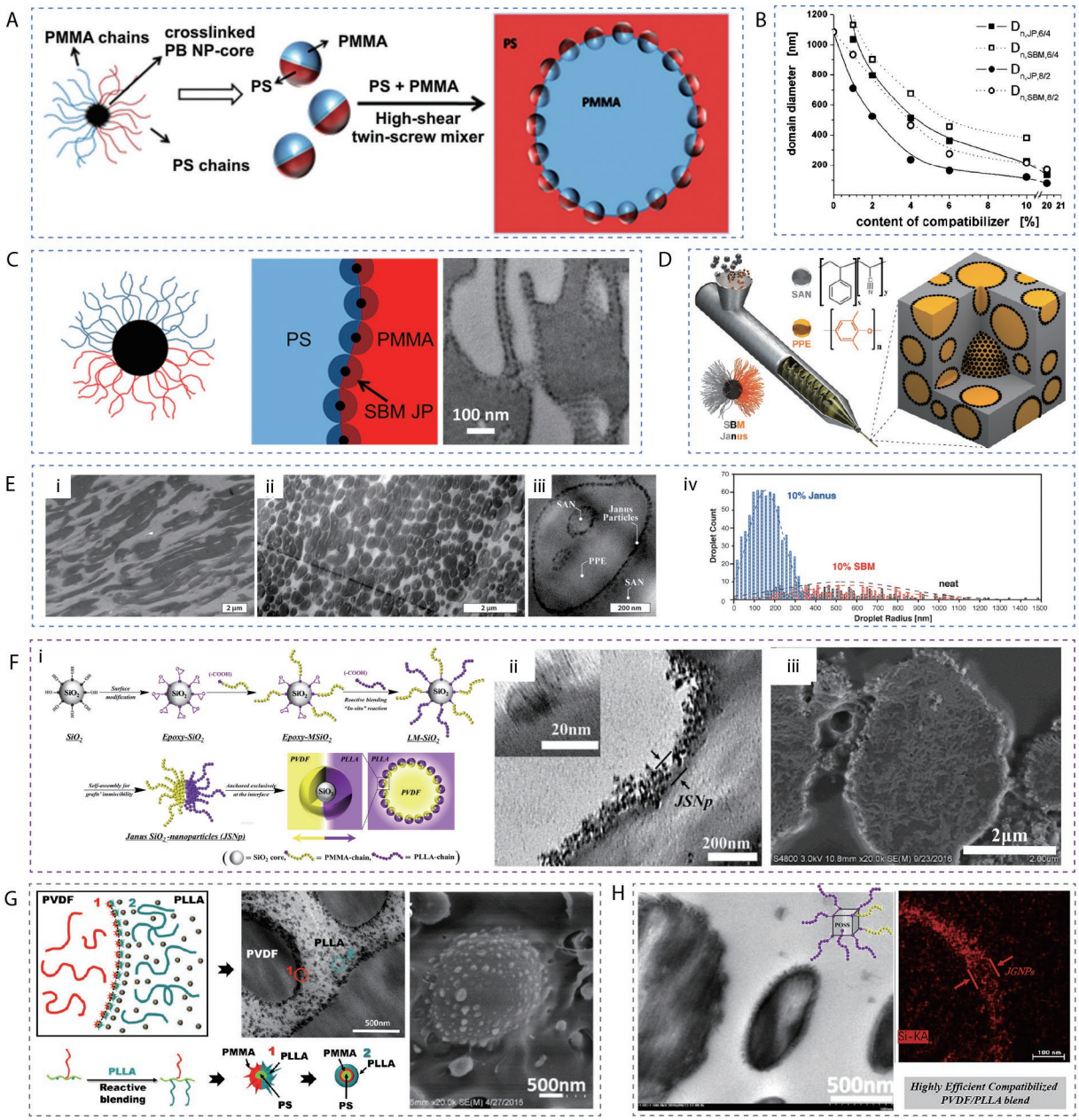

Fig. 4 (A) Schematic diagram of spherical Janus particles and their adsorption at the blend interface of a PS/PMMA blend subjected to a high-shear mixing.[42] (B) Variation of PMMA discrete domain diameter with the compatibilizer content of SBM ternary block copolymer and Janus particles for different blending ratios. (Reprinted with permission from Ref. [42], Copyright (2008) American Chemical Society). (C) Schematic and TEM micrograph of the SBM JNPs with cross-linked PB cores (black) and grafted PS (blue) and PMMA (red) chains densely assembling at the PS/PMMA interface. (Reprinted with permission from Ref. [58], Copyright (2015) American Chemical Society). (D) Processing diagram of SAN/PPE blends using SBM JNPs as compatibilizer, JNPs (black dots) stabilizing PPE droplets (yellow) within SAN matrix (gray) [59]. (E) TEM morphologies of PPE (dark)/SAN (bright) blend (60/40, *W*/*W*), (i) without and (ii) with 10 wt% of SBM JNPs, (iii) TEM magnification of double emulsion droplet shows JNPs (black dots) exclusively located at the PPE/SAN blend interface, (iv) Histogram of droplet radius for neat blend and blends filled with SBM triblock terpolymer or SBM JNPs. (Reprinted with permission from Ref. [59], Copyright (2014) American Chemical Society). (F) (i) Schematic diagram of in situ formation of Janus SiO_2 nanoparticles from the epoxy groups modified SiO_2 by reactive blending [60], (ii) TEM images of PLLA/PVDF blend with Janus SiO_2 nanoparticles encapsulating at interface, (iii) SEM image demonstrating thermodynamic stability of binary phase morphology suffering from thermal annealing (200 °C for 20 min). (Reprinted with permission from Ref. [60], Copyright (2017) American Chemical Society). (G) *In situ* formation of Janus nanomicelles for compatibilizing the PLLA/PVDF blend. SEM image of the PLLA/PVDF blend with 3 phr P((S-*co*-GMA)-*g*-MMA). (Reprinted with permission from Ref. [61], Copyright (2015) American Chemical Society). (H) TEM and elemental mapping images of PLLA/PVDF (50/50) blend with POSS Janus particles (PLLA-premixed sequence). (Reprinted with permission from Ref. [63], Copyright (2017) Elsevier Ltd.).

https://doi.org/10.1007/s10118-022-2878-y

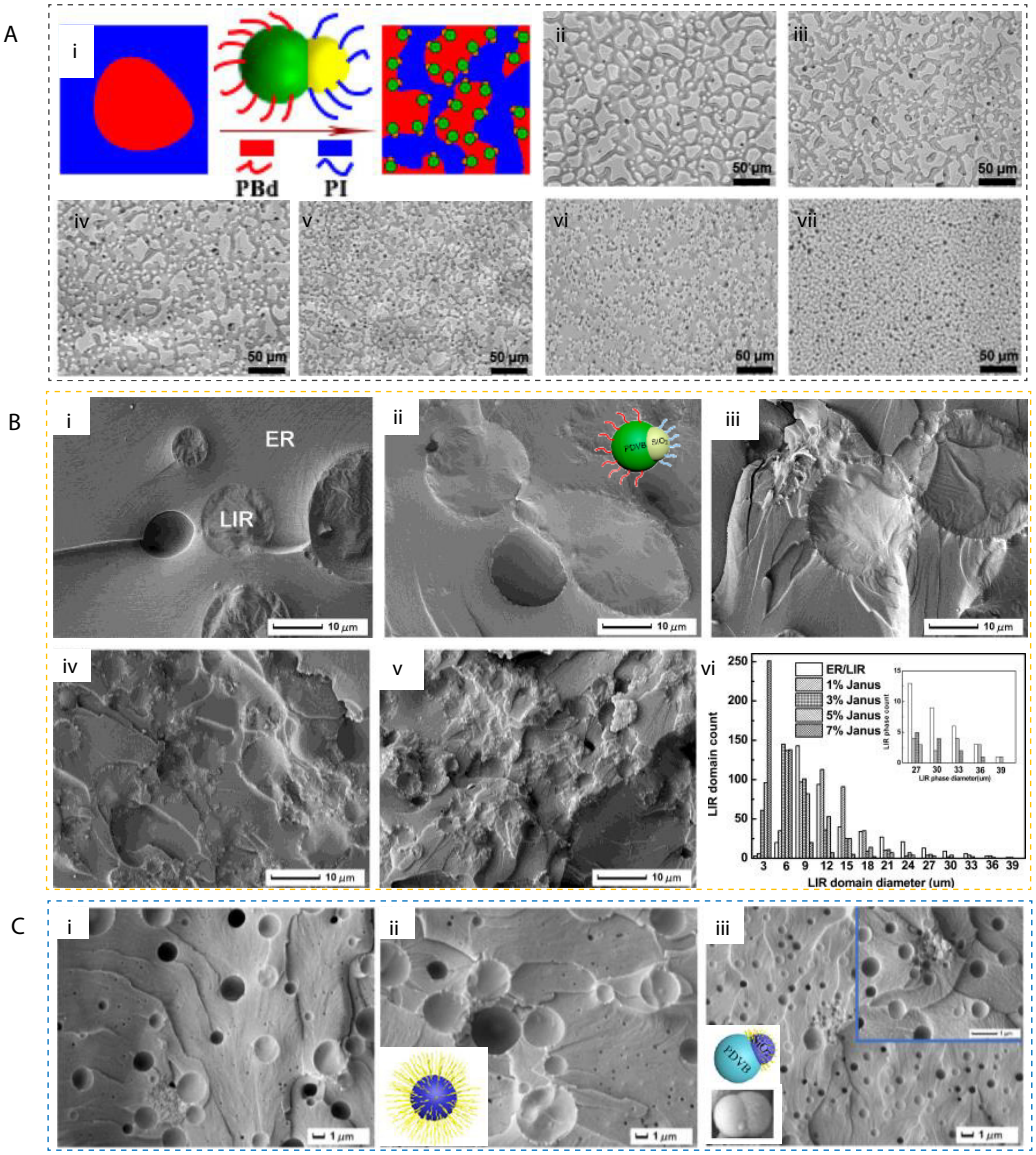

Fig. 5 Changes of domain size and shape for snowman-like Janus particles as compatibilizers of blends. (A) (i) Diagram of snowman-like Janus rubber hybrid particles (PI-SiO_2@PDVB-PBd) as compatibilizer of PI/PBd blend. Phase contrast optical microscopic images of the PI/PBd (6/4, *W*/*W*) blends filled with Janus particles of varied contents: (ii) 0 wt%, (iii) 0.93 wt%, (vi) 1.85 wt%, (v) 2.22 wt%, (vi) 2.8 wt%, and (vii) 5.55 wt% (The light gray and dark gray phases are PBd and PI domain, respectively. The black dots are Janus particles.) (Reprinted with permission from Ref. [64], Copyright (2016) American Chemical Society). (B) SEM images of fracture surface of LIR/ER blends without (i) and with (ii) 1%, (iii) 3%, (iv) 5%, (v) 7% snowman-like MPS-SiO_2@PDVB-DM Janus particles, (vi) LIR domain sizes of blends with varied Janus particles contents. (Reprinted with permission from Ref. [65], Copyright (2017) American Chemical Society). (C) SEM images of fracture surface of AR/EP blends filled with (i) 2 wt% SiO_2, (ii) SiO_2-TETA, and (iii) TETA-SiO_2@PDVB S-JNPs. (Reprinted with permission from Ref. [66], Copyright (2019) American Chemical Society).

polystyrene/polyamide-6 (PS/PA6) melt blend.[67,68] Furthermore, Yu *et al*. found that the S-JNPs could widen the composition range of blend for cocontinuous morphology, realizing a cocontinuity in immiscible blends by adding only 0.9 vol% S-JNPs.[69]

The aforementioned studies revealed that the snowman-like Janus nanoparticles used to realize a desirable interfacial compatibilizing for immiscible blends are generally by grafting polymer chains or modifying surface of S-JNPs, which complicates the fabricating process. On this account, Liang *et al*. proposed a more simple and feasible strategy to localize the S-JNPs at blend interfaces, namely tailoring the intrinsic characteristics of S-JNPs, the Janus balance (*J*).[70] For S-JNPs with a specific chemical component, its *J* value is determined by the shape anisotropy (ratio of two lobe size). Hence, the interfacial properties of immiscible blends can be tailored by simply altering the two-lobe size ratio of S-JNPs. In this study, the snowman-like PS/PBA@Silica (poly(*n*-butyl acrylate), PBA) JPs with four varied two-lobe size ratios were synthesized and applied to compatibilize the poly(lactic acid)/poly(butylene succinate) (PLA/PBS) (80/20, *W*/*W*) biodegradable blend (Fig. 6A). With the size ratios of the silica and PS/PBA lobes de-

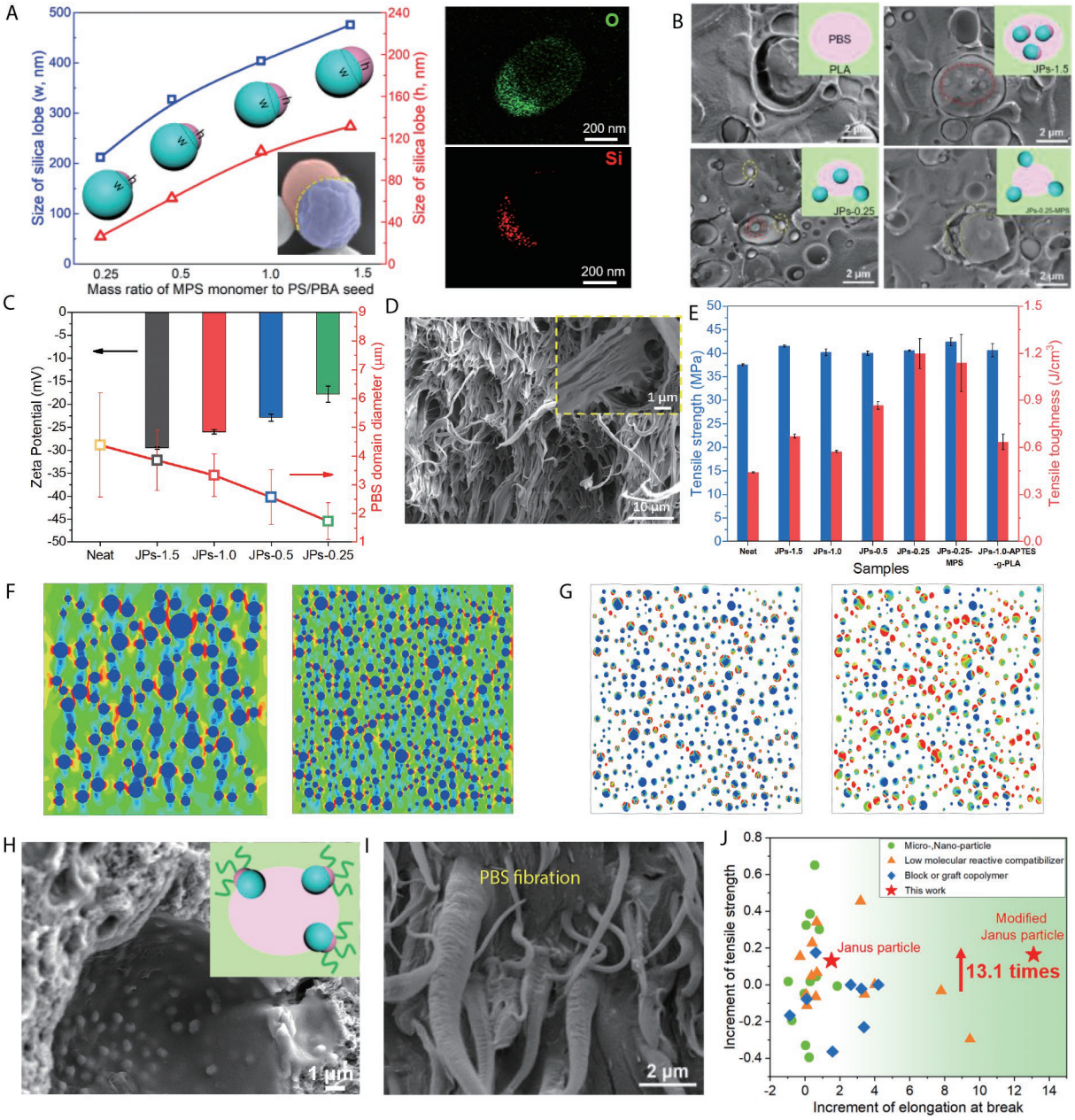

Fig. 6 (A) Morphology evolution of snowman-like PS/PBA@Silica Janus nanoparticles with various sizes of silica lobe as a function of mass ratios of MPS monomer and PS/PBA seed. Inset SEM image and EDX elemental mapping images of the S-JNPs-1.0 sample. (B) Controllable migration of S-JNPs compatibilizers in the PLA/PBS blends from PBS discrete phase to the interface. (C) PBS domain diameter generally decreasing as the S-JNPs with increased zeta potential migrating to the interface. (D) SEM images of ductile fracture surface after tensile loading of PLA/PBS (80/20, *W*/*W*) composite with S-JNPs located at interface. (E) Tensile strength and toughness of PLA/PBS/S-JNPs blends. (F) Mises stress distribution of PLA/PBS blends with S-JNPs located at PBS phase (left) and interface (right), respectively (tensile strains ε=0.028). (G) Plastic deformation (characterized by equivalent plastic strain, PEEQ) of PLA/PBS/JPs-0.25 with interface strength of 5 MPa (left) and 10 MPa (right). (H) SEM image of PLA/PBS blend filled with epoxy group modified S-JNPs after etching PBS droplets, demonstrating a single layer arrangement of S-JNPs along the PLA/PBS interface. (I) SEM image of tensile fracture surface of PLA/PBS blend filled with epoxy group modified S-JNPs showing intense fibration of flexible PBS domains. (J) Superiority of modified S-JNPs on increments of tensile strength and elongation at break of blend to other different types of compatibilizers. (Reprinted with permission from Ref. [70], Copyright (2022) American Chemical Society).

creasing, the JPs could migrate from the dispersed PBS domains to the interface, and even completely locate at the interfaces by adjusting the zeta potential of JPs (Fig. 6B), meanwhile, the domain diameters of dispersed phases generally reduce (Fig. 6C). The selective location of the JPs at the blend interface plays a preferable compatibilizing effect, transforming the brittle fracture of blend to a ductile fracture (Fig. 6D), and significantly enhancing the tensile toughness of blend (Fig. 6E). Moreover, the numerical computation based on two-dimensional (2D) finite-element model was carried out as

well. It was revealed that the compatibilizing effect of refining the dispersed phase size contributed to the uniform stress distribution of blend under loading, thus delaying fracture of of blend (Fig. 6F). The numerical results also indicated that enhancing interfacial adhesion between two components of blend played a more significant role on the improvement of mechanical properties, *e.g.*, facilitating the plastic deformation of flexible PBS domains, thus improving the tensile toughness of the blend (Fig. 6G). To further increase the toughness of blend by enhancing interfacial strength, the epoxy groups was grafted onto the silica lobe of PS/PBA@Silica JPs. These epoxy groups of JPs located at interface reacted with PLA chains in the PLA matrix during melt blending, which greatly increased the interfacial adhesion (Fig. 6H), thus inducing the intense fibration of flexible PBS domains (Fig. 6I) under tensile loading. This significantly improved the elongation at break of blend beyond current various compatibilizers of PLA/PBS blends (Fig. 6J). The snowman-like Janus particle is of great potential in the compatibilization of immiscible blend.

Compatibilization of Janus nanosheets

Differing from the Janus nanoparticles, the two-dimensional Janus nanosheets (JNSs) could stabilize the polymeric interfaces by forming a jamming structure. He *et al*. grafted the PS and PI polymer chains on two sides of silica nanosheets (20 nm thick), respectively, to synthesize the PS-silica-PI Janus nanosheets.[71] As the compatibilizer of PS/PI blend, the PS-silica-PI JNSs significantly reduced the phase domain sizes of blend (Fig. 7A), and weakened the phase domain coarsening induced by the annealing (Fig. 7A, ii and iii). In addition, PBd-silica-PI JNSs were also fabricated to compatibilize the blend of solution styrene-butadiene rubber/natural rubber (SSBR/NR).[72] The interfacial location of PBd-silica-PI JNSs not only facilitated the formation of bicontinuous structure, but also decreased the SSBR phases domain size. Except for silica JNSs, the layered silicate kaolinites with two opposing tetrahedral surfaces (TS) and octahedral (OS) surfaces were chemically modified to Janus sheets by attaching polymer chains on distinct functional groups of TS and OS, respectively.[73] Besides, these formed JNs could selectively assemble at the interface of the PS/PMMA blend. Li *et al*. designed the regularly shaped hexagonal gibbsite nanosheets into JNSs by *in situ* generating PLLA and poly(butylene succinate) (PBSU) chains on the nanosheet surfaces during melt blending (Fig. 7B, i and ii).[74] They found that the rigid JNs located at the PLLA/PBSU interface could change the geometries of PBSU domains from spherical shapes to irregular shapes (Fig. 7B, iii). And even the PBSU domains were distorted to strip shapes at JNs loading content of 5 wt%, resulting in the size of PBSU domains decreasing drastically (Fig. 7B, iv).

In addition to decreasing the size of dispersed phase for polymer blend, Janus nanosheets are more effective to enhance microstructural stability and mechanical properties of the compatibilized polymer blends. The JNS with epoxide group and nitrile-butadiene rubber (NBR) on its opposite sides (denoted as EP/NBR JNS) was also applied to compatibilize the epoxy resin/liquid nitrile-butadiene rubber (EP/LNBR).[11] It was found that the JNSs were exclusively located at the interface of EP/LNBR blend under a fluorescence microscope (FM) (Fig. 7C, i) and TEM (Fig. 7C, ii), and the interfacial coverage by the JNSs reached a saturated state at only 0.20 phr of JNSs (Fig. 7C, iii and iv). Meanwhile, the introduction of 0.20 phr JNSs realized a synchronously strengthening and toughening of EP/LNBR blend (Fig. 7D), resulting from a single layer of JNSs anchored at interface effectively transferring stress between EP and LNBR (Fig. 7E, i and ii). When the JNSs content is above the saturated interfacial coverage (*i.e.*, 0.4 phr), the stack of multiple layers of JNSs at the interface weakens the interfacial adhesion (Fig. 7E, iii and iv), impairing the stress transferring efficiency, further the mechanical properties of EP/LNBR/0.4 phr JNSs decreasing (Fig. 7D).

Due to irregular sheet microstructure of Janus nanosheets, the JNSs can form a jamming structure at a very low threshold. Our group synthesized the PMMA/epoxy JNS and used it as compatibilizer of PVDF/PLLA (60/40, *W*/*W*) (Fig. 8A).[12] It was observed that only adding 0.5 wt% of JNS could achieve a saturated interfacial coverage (Fig. 8B), and form an interconnected jamming structure (Fig. 8C). Profiting from stabilizing effect of the jamming structure, a robust PVDF porous material can be derived after selectively etching PLLA (Fig. 8D), and be held well even suffering from high temperature annealing (Fig. 8E). Moreover, the interfacial stability was further verified by filling carbon black within the channel to build a continuous conducting network. After compressing at 190 °C, the conducting network and conductivity were well preserved in the case of filling 0.5 wt% JNS, which was attributed to the interfacial stabilization of JNS armored at the pore skeleton surface (Fig. 8F). Furthermore, the mechanical properties and gas barrier performance of a biodegradable PLA/PBS blend using JNSs as compatibilizer were also investigated (Fig. 8G).[75] The organic–inorganic PLA/PBS Janus nanosheets can jam at the interface of the PLA/PBS blend at a low threshold of 0.5 wt% (Fig. 8H), and the tensile strength and elongation at break of the PLA/PBS blend are significantly improved. After hot pressing, the PLA/PBS/0.5 wt% JNS composite membrane yet displays a desirable gas barrier performance (Fig. 8I). Causally, the large aspect ratio of PBS domains forms a layered structure inside PLA/PBS composites by pressing, and a dense silica layer is built by the PLA/PBS JNs located at the interface.

Numerical Simulation of Janus Particle as Compatibilizer

To elucidate more comprehensively the compatibilizing effect of Janus particles for immiscible blends, the numerical simulation based on various methods have been developed. For example, Guo *et al*. compared the different effects of Janus and homogeneous nanospheres on the phase separation dynamics of polymer blends using dissipative particle dynamics (DPD) method (Fig. 9A).[76] It is obtained that the phase separation dynamics of blend systems with Janus nanospheres is slower, and these Janus nanospheres can effectively impede domain growth, prompting formation of smaller size domain at later stages of the phase separation process. This results from the inherent equatorial adsorption and low desorption probability of Janus nanostructures at the blend interface, which contribute to significantly decreasing the interfacial tension, and thus reducing the driving force to induce macrophase separation. Moreover, they also investigated the phase behavior and phase dynamics of blend systems

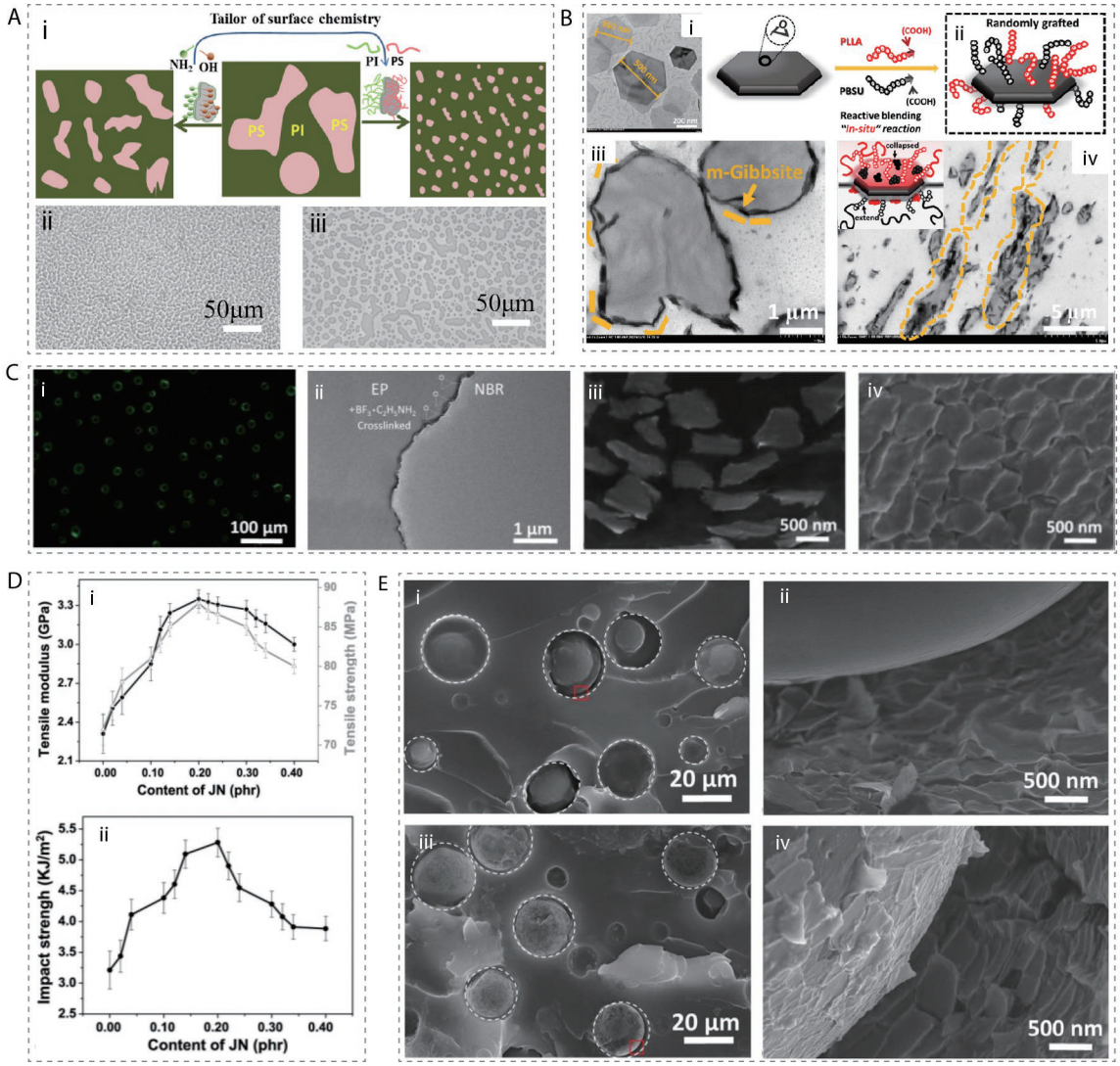

Fig. 7 Compatibilization of Janus nanosheets for different blends. (A) (i) Schematic illustrating the effect of surface modification of silica nanosheets on compatibilization for PS/PI blends. Optical microscopic images of the PS/PI (6/4, *W*/*W*) blend filled with PS-silica-PI Janus nanosheets: (ii) as-prepared film and (iii) film annealed at 150 °C for 60 min. (Reprinted with permission from Ref. [71], Copyright (2018) American Chemical Society). (B) (i) TEM images of hexagonal gibbsite nanoplatelets, (ii) Diagram of *in situ* formation of the randomly binary grafted nanoplates by reactive blending, (iii) TEM image of PLLA/PBSU (70/30) blend with 3 wt% modified gibbsite (m-gibbsite) at the interface, (iv) TEM image of PLLA/PBSU/m-gibbsite (70/30/5) indicating the rigid JNs located at the interface changing the geometries of PBSU domains to strip shape. (Reprinted with permission from Ref. [74], Copyright (2022) American Chemical Society). (C) (i) Fluorescence microscopy image of the EP/LNBR blend with 0.20 phr JNSs located at the interface (FITC-labeled JNs displaying green) [11], (ii) cross-sectional TEM image of the blend, SEM images of the blends filled with (iii) 0.02 and (iv) 0.20 phr JNSs. (D) Mechanical properties, (i) tensile modulus and strength, (ii) impact strength) of blends as a function of JNSs content. (E) SEM image of tensile fractured surface of EP/LNBR with (i and ii) 0.2 phr and (iii and iv) 0.4 phr JNSs. (Reprinted with permission from Ref. [11], Copyright (2019) American Chemical Society).

containing Janus nanoparticles with different shapes (including Janus nanospheres, nanodiscs and nanorods) and dividing surface ("standing" and "lying" particles) (Fig. 9B).[77] They demonstrated that only the anisotropic "standing" Janus nanostructures is conducive to the formation of a lamellar phase in blend system. And the compatibilizing efficiency of Janus nanostructures is also relevant to their total dividing surface area (depending on particle shapes and dividing surface designs). Furthermore, they explored the influences of nanorods with three typical surface properties on the compatibilization performance and phase morphologies of polymer blend.[78] Comparing with homogeneous nanorods, the Janus nanorods can strongly adsorb at the interface even undergoing the shear load, and displaying a lateral ordering in a shear-induced lamellar phase with a parallel orientation (Fig. 9C). Zhou *et al.* also studied the effect of Janus nanorods on interfacial tension of polymer blend utilizing the DPD method.[79] It showed that the length of Janus nanorods can determine their orientation, *e.g.*, the shorter Janus nanorods tending to "standing", thus further influencing the interfacial

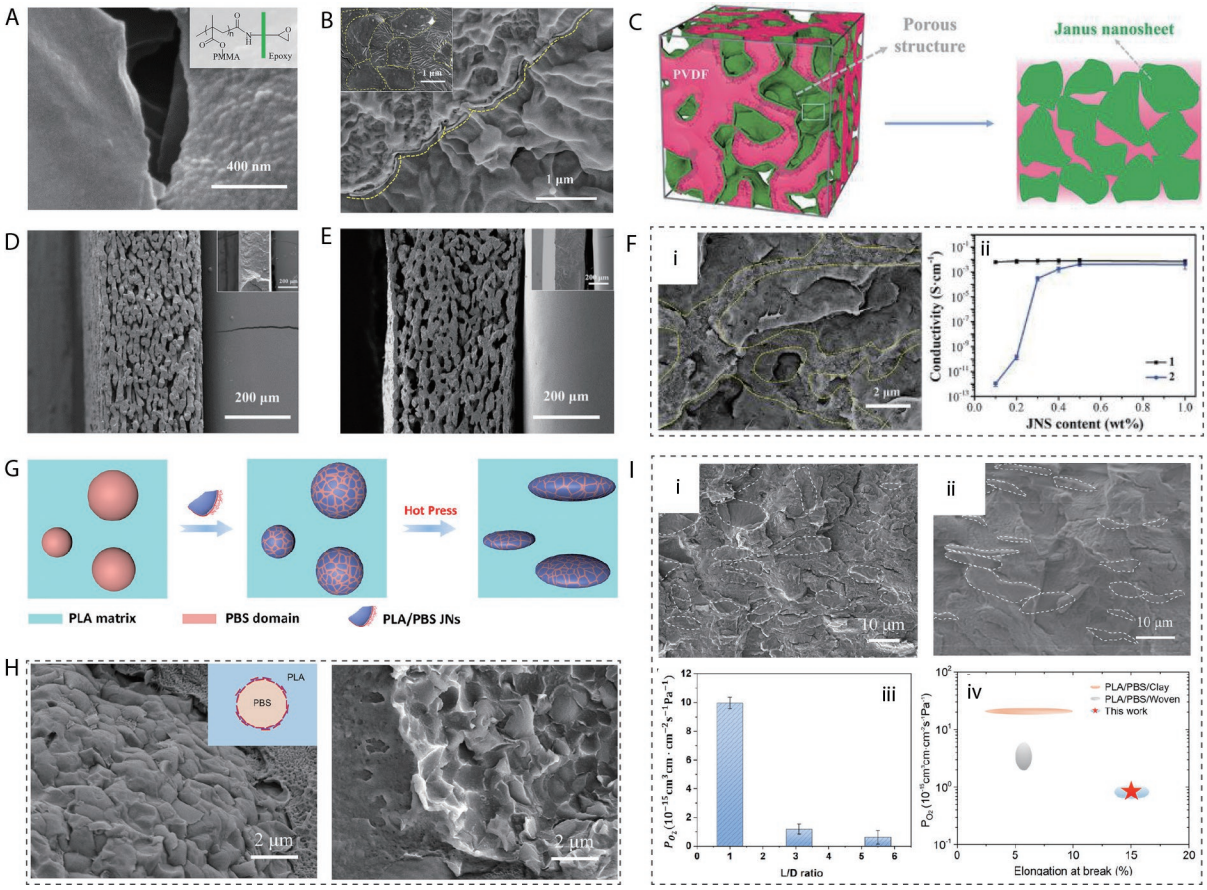

Fig. 8 (A) SEM image of Janus nanosheets decorated by PMMA and epoxy. (B) SEM image of the PVDF/PLLA blend filled with 0.5 wt% PMMA/epoxy JNSs showing an interfacial jamming structure. (C, D) Interfacial stabilization of PVDF/PLLA blend by the jamming of PMMA/epoxy JNSs facilitating to form a porous structure after selectively etching PLLA. (E) SEM image of the maintained porous structure after suffering from the annealing at 190 °C for 30 min. (F) The compressed blend with 0.5 wt% JNSs preserving a conducting network (i) cross-sectional SEM image and (ii) conductivity (1. PVDF/CB composites, 2. PVDF/PLLA/JNSs blend after compressing at 190 °C). (Reprinted with permission from Ref. [12], Copyright (2020) John Wiley and Sons). (G) Schematic of interfacial stabilization of the PLA/PBS blend by the PLA/PBS JNSs acting as compatibilizer and formation of flat PBS domains after hot-pressing. (H) SEM images of cryofracture surfaces of PLA/PBS (70/30, *W*/*W*) blend with 0.5 wt% PLA/PBS JNSs. (I) Oxygen barrier properties of PLA/PBS/JNSs blends. SEM images of PLA/PBS/0.5 wt % JNs blend at (i) 35 and (ii) 50 bar pressure, (iii) oxygen permeability (P_{O_2}) of PLA/PBS membrane with different aspect ratios of PBS domains by hot pressing of varied pressures, (iv) comparison of P_{O_2} and elongation at break with other PLA/PBS materials. (Reprinted with permission from Ref. [75], Copyright (2022) American Chemical Society).

tension of blend. Estridge and Jayaraman used the coarse-grained molecular simulations to study the compatiblizing effects of AB diblock copolymer grafted particles (DBCGPs) and Janus homopolymer grafted particles (JGPs) for immiscible blend of A and B homopolymers.[80] The numerical results showed that the JGPs could exactly locate at the interface of A/B blend, while the DBCGPs centers were off the interface for maximizing the contacts between the grafted block of DBCGP and blend. (Fig. 9D, i). More notably, the JGPs had the largest desorption energy for leaving the interface (Fig. 9D, ii) and most significant reduction in interfacial tension (Fig. 9D, iii) in comparison with DBCGPs and diblock copolymers. These result in the great stability of JGPs at the interface of A/B blend to realize the significant compatibilization. Yan *et al.* investigated the structural morphologies and kinetics of binary polymer blends filled with one-dimensional Janus nanorods during shear and relaxing after ceasing shear using cell dynamics system (CDS) method (Fig. 9E, i).[81] They found that the shear force could promote the uniform alignment of Janus nanorods at the interface of blend (Fig. 9E, iii), and their angles along the interface is related to the ratio between two surface chemical compartments of Janus nanorods (Fig. 9E, ii). Moreover, the distinctive phase morphologies, *e.g.*, orientationally hierarchical structures, can be attained during shear process (Fig. 9E, iii) and be arrested in the relaxing process after ceasing shear (Fig. 9E, iv) by adjusting the surface geometry of Janus nanorods.

CONCLUSIONS AND OUTLOOK

In this review, we outlined the recent advantage application of Janus particles as compatibilizers for the interfacial engineering of polymer blend. As amphiphilic particles, Janus particles integrate the selective interaction abilities of diblock copolymers and Pickering effect of nanoparticles, and can act as efficient compatibilizers of immiscible blends. They can refine

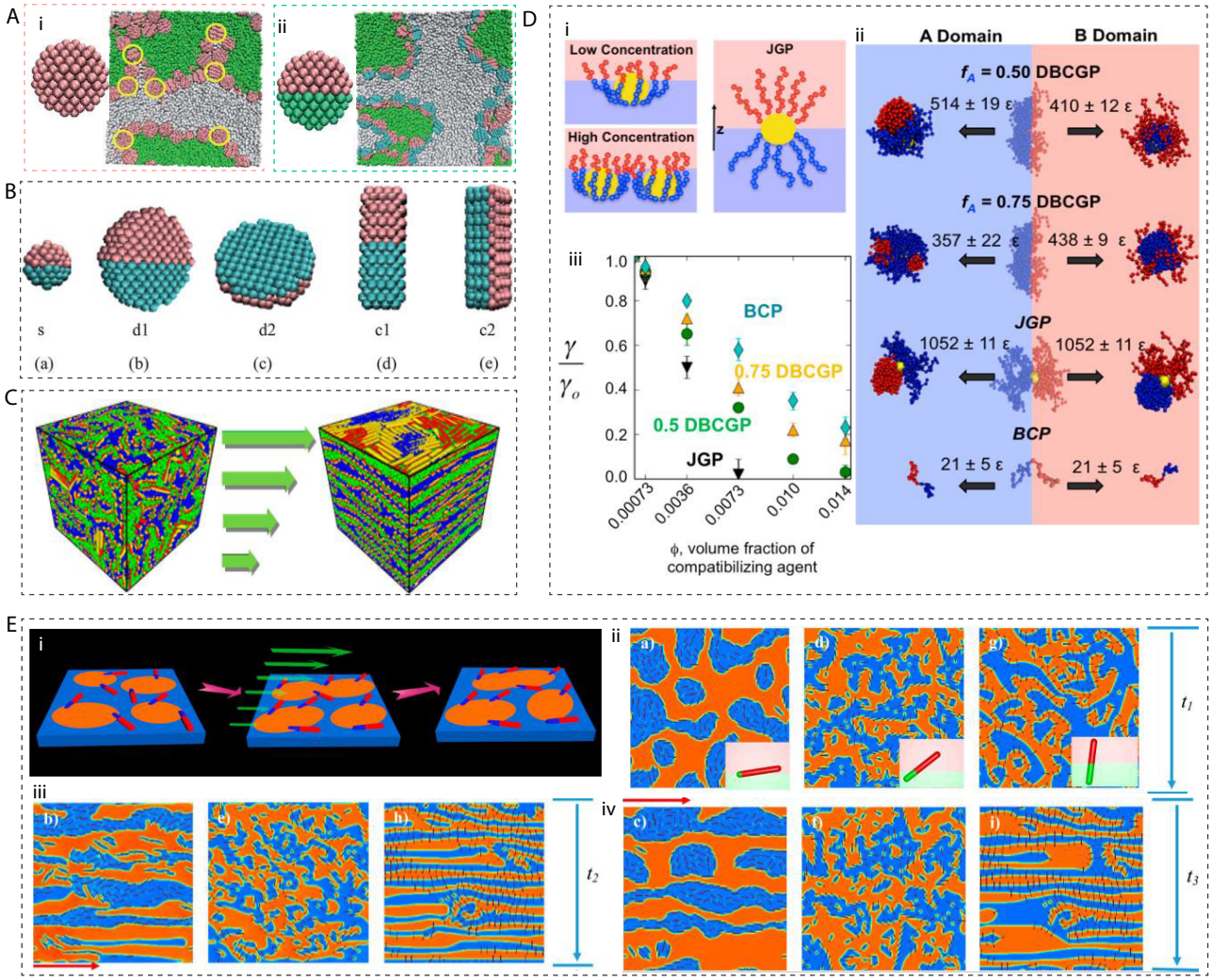

Fig. 9 (A) Two regions selected from the snapshots showing homogeneous nanospheres are not always equatorially adsorbed at the interfaces (i), while Janus nanospheres are almost adsorbed equatorially at interfaces (ii). (Reprinted with permission from Ref. [76], Copyright (2012) The Royal Society of Chemistry). (B) Three shapes of Janus nanoparticles (nanospheres, nanodiscs, and nanorods) used in simulations revealing the relation between compatibilizing efficiency and dividing surface area of different Janus nanostructures. (Reprinted with permission from Ref. [77], Copyright (2013) The Royal Society of Chemistry). (C) Janus nanorods adsorbed at the interface inducing a lamellar phase undergoing the shear load. (Reprinted with permission from Ref. [78], Copyright (2018) American Chemical Society). (D) (i) Schematics of DBCGP and JGP configurations at the interface, (ii) Configurations of various compatibilizers and the corresponding desorption energies, (iii) ratio of interfacial tension of compatibilized blend (γ) to compatibilizer-free blend (γ_0) with ϕ varying. (Reprinted with permission from Ref. [80], Copyright (2015) American Chemical Society). (E) (i) Schematic diagram illustrating three stages of the research, including self-assembly (left), shearing (middle), and relaxing stage (right). Morphologies of binary polymer blends filled with Janus nanorods at the end of three stages with time t_1, t_2 and t_3, respectively, are as follows: (ii) self-assembly stage, (iii) shearing stage, and (vi) relaxing stage. (The red arrow in iii) indicates the direction of shear flow). (Reprinted with permission from Ref. [81], Copyright (2013) American Chemical Society).

dispersed phases due to the combined dual roles of copolymers and nanoparticles, and stabilize blend morphologies once the JPs migrate to the interface between the two polymer blends. Meanwhile, their amphiphilic balance (Janus balance) can be easily adjusted by their surface area, shape and compositions.

An efficient interfacial tailoring strategy for immiscible blends may have far-reaching implications for exploitation and multifunctional applications of high-performance polymers alloys for different engineering fields. Although Janus particles have been demonstrated excellent performance as compatibilizers to broadly control the phase structure and mechanical properties of the polymer blend, it is noteworthy that some challenges remain in many areas. First, efficient methodologies for precise large-scale synthesis of Janus particles remain challenging. Second, Janus particles with soft and hard segments are more effective to enhance interfacial mechanical properties. Therefore, both its internal and surface composition design are important. Third, it is urgent to develop a new theory for interfacial behavior of Janus particles, which is different from molecular surfactants. Forth, apart from the compatibilization, the Janus particles that could endow immiscible polymer blends with more functionalities (*i.e.*, electrical or thermal conductivity, flame retardancy, *etc.*) should be developed, especially realizing that at a

very low threshold.

BIOGRAPHY

Fu-Xin Liang received his Ph.D. degree from Institute of Chemistry, Chinese Academy of Sciences (ICCAS) in 2011. He started his academic career at ICCAS from assistant professor (2011–2013) to associate professor (2013–2017) to professor (2017–2019). In 2019, he joined the Department of Chemical Engineering at Tsinghua University as an associate professor. His research works focus on design of amphiphilic Janus materials and their application in polymer composite such as polymer blends, and functional coating.

NOTES

The authors declare no competing financial interest.

ACKNOWLEDGMENTS

This work was financially supported by the National Natural Science Foundation of China (Nos. 52173076 and 52042302), China Postdoctoral Science Foundation (No. 2021M701825), Tsinghua-Foshan Innovation Special Fund (TFISF) (No. 2021THFS0212), and Joint Agency Affiliate Projects of China Petroleum & Chemical Corporation (No. 20212930037).

REFERENCES

1 Cardinale's, R.; Moldenaers, P., in *Morphology development in immiscible polymer blends. Polymer Morphology: Principles, Characterization and Properties*, Ed. by Guo, Q., John Wiley & Sons, **2016**; Chapter 19, pp. 348-373.
2 Thomas, S.; Grohens, Y.; Jyotishkumar, P., in *Characterization of polymer blends: miscibility, morphology and interfaces*, John Wiley & Sons, **2014**; Chapter 1, pp. 1–3.
3 Sinha Ray, S.; Bousmina, M. Compatibilization efficiency of organoclay in an immiscible polycarbonate/poly(methyl methacrylate) blend. *Macromol. Rapid Commun.* **2005**, *26*, 450–455.
4 Utracki, L. A. Compatibilization of polymer blends. *Can. J. Chem. Eng.* **2002**, *80*, 1008–1016.
5 Elias, L.; Fenouillot, F.; Majesté, J. C.; Alcouffe, P.; Cassagnau, P. Immiscible polymer blends stabilized with nano-silica particles: rheology and effective interfacial tension. *Polymer* **2008**, *49*, 4378–4385.
6 Dai, K. H.; Kramer, E. J.; Shull, K. R. Interfacial segregation in two-phase polymer blends with diblock copolymer additives: the effect of homopolymer molecular weight. *Macromolecules* **1992**, *25*, 220–225.
7 Wang, X. F.; Zhang, Z. X.; Yang, J. H.; Wang, Y.; Zhang, J. H. Largely improved fracture toughness of an immiscible poly(L-lactide)/ethylene-*co*-vinyl acetate blend achieved by adding carbon nanotubes. *RSC Adv.* **2015**, *5*, 69522–69533.
8 Liang, F. X.; Zhang, C. L.; Yang, Z. Z. Rational design and synthesis of Janus composites. *Adv. Mater.* **2014**, *26*, 6944–6949.
9 Jiang, S.; Chen, Q.; Tripathy, M.; Luijten, E.; Schweizer, K. S.; Granick, S. Janus particle synthesis and assembly. *Adv. Mater.* **2010**, *22*, 1060–1071.
10 Cardinaels, R., in *Compatibilization of polymer blends: micro and nano scale phase morphologies, interphase characterization, and properties*, eds. by Ajitha, A. R., Thomas, S., Elsevier, Netherlands, **2020**, Chapter 8, p. 253–270.
11 Hou, Y.; Zhang, G. L.; Tang, X. P.; Si, Y.; Song, X. M.; Liang, F. X.; Yang, Z. Z. Janus nanosheets synchronously strengthen and toughen polymer blends. *Macromolecules* **2019**, *52*, 3863–3868.
12 Guan, J. P.; Gui, H. G.; Zheng, Y. Y.; You, J. C.; Li, Y. J.; Liang, F. X.; Yang, Z. Z. Stabilizing polymeric interface by Janus nanosheet. *Macromol. Rapid Commun.* **2020**, *41*, 2000392.
13 Sharifzadeh E. Modeling of the mechanical properties of blend based polymer nanocomposites considering the effects of Janus nanoparticles on polymer/polymer interface. *Chinese J. Polym. Sci.* **2019**, *37*, 164–177.
14 Robeson, L. M. Polymer blends. A comprehensive review, **2007**, 641.
15 Paul, D. R. *Polymer Blends*. Volume 1 (Vol. 1). Elsevier, **2012**.
16 Paul, D. R.; Barlow, J. W. A binary interaction model for miscibility of copolymers in blends. *Polymer* **1984**, *25*, 487–494.
17 Djordjevic, M. B.; Porter, R. S. NMR characterization of intermolecular interactions for polymers, IV. Intermolecular interactions of low molecular weight analogues for compatible blends of polystyrene and poly(2,6-dimethyl-1,4-phenylene oxide). *Polym. Eng. Sci.* **1983**, *23*, 650–657.
18 Tjong, S. C.; Meng, Y. Z. Effect of reactive compatibilizers on the mechanical properties of polycarbonate/poly(acrylonitrile-butadiene-styrene) blends. *Eur. Polym. J.* **2000**, *36*, 123–129.
19 Macosko, C. W., in *Morphology development and control in immiscible polymer blends*. In Macromolecular Symposia, Vol. 149, WILEY-VCH Verlag, Weinheim, **2000**, p. 171
20 Pötschke, P.; Paul, D. R. Formation of co-continuous structures in melt-mixed immiscible polymer blends. *J. Macromol. Sci.-Polym. Rev* **2003**, *43*, 87–141.
21 Lyngaae-Jørgensen, J.; Utracki, L. A. in *Dual phase continuity in polymer blends*. In Makromolekulare Chemie. Macromolecular Symposia, Basel: Hüthig & Wepf Verlag, **1991**, p. 189
22 He, J.; Bu, W.; Zeng, J. Co-phase continuity in immiscible binary polymer blends. *Polymer* **1997**, *38*, 6347–6353.
23 Li, Y.; Shimizu, H. Novel morphologies of poly(phenylene oxide)(PPO)/polyamide 6 (PA6) blend nanocomposites. *Polymer* **2004**, *45*, 7381–7388.
24 Metelkin, V. I.; Blekht, V. S. Formation of a continuous phase in heterogeneous mixtures of polymers. *Kolloidnyi Zhurnal* **1984**, *46*, 476–480.
25 Kozlowski, M. The formation of interpenetrating polymer blends. *J. Polym. Eng.* **1995**, *14*, 15–40.
26 Noolandi, J.; Hong, K. M. Interfacial properties of immiscible homopolymer blends in the presence of block copolymers. *Macromolecules* **1982**, *15*, 482–492.
27 Zhang, J. B.; Ji, S. X.; Song, J.; Lodge, T. P.; Macosko, C. W. Flow accelerates interfacial coupling reactions. *Macromolecules* **2010**, *43*, 7617–7624.
28 Koning, C.; Duin, M. V.; Pagnoulle, C.; Jerome, R. Strategies for compatibilization of polymer blends. *Prog. Polym. Sci.* **1998**, *23*, 707–757.
29 Bell, J. R.; Chang, K.; López-Barrón, C. R.; Macosko, C. W.; Morse, D. C. Annealing of cocontinuous polymer blends: effect of block copolymer molecular weight and architecture. *Macromolecules* **2010**, *43*, 5024–5032.
30 Zhao, X. W., *Surface modification of carbon nanoparticles and the compatibilization effects on PVDF/PLLA blends*, Thesis, Hangzhou Normal University, **2019**.
31 Su, S.; Kopitzky, R.; Tolga, S.; Kabasci, S. Polylactide (PLA) and its blends with poly(butylene succinate) (PBS): a brief review. *Polymers* **2019**, *11*, 1193.
32 He, L.; Song, F.; Li, D. F.; Zhao, X.; Wang, X. L.; Wang, Y. Z. Strong and tough polylactic acid based composites enabled by

simultaneous reinforcement and interfacial compatibilization of microfibrillated cellulose. *ACS Sustain. Chem. Eng.* **2020**, *8*, 1573–1582.
33 Chen, G. X.; Kim, H. S.; Kim, E. S.; Yoon, J. S. Compatibilization-like effect of reactive organoclay on the poly(L-lactide)/poly(butylene succinate) blends. *Polymer* **2005**, *46*, 11829–11836.
34 Wu, W.; Wu, C. K.; Peng, H. Y.; Sun, Q. J.; Zhou, L.; Zhuang, J. Q.; Cao, X. W.; Roy, V. A. L.; Li, R. K. Y. Effect of nitrogen-doped graphene on morphology and properties of immiscible poly(butylene succinate)/polylactide blends. *Compos. Pt. B-Eng.* **2017**, *113*, 300–307.
35 Tan, L. C.; He, Y.; Qu, J. P. Structure and properties of Polylactide/poly(butylene succinate)/organically Modified Montmorillonite nanocomposites with high-efficiency intercalation and exfoliation effect manufactured *via* volume pulsating elongation flow. *Polymer* **2019**, *180*, 121656.
36 Wang, X. M.; Zhuang, Y. G.; Dong, L. S. Study of carbon black-filled poly(butylene succinate)/polylactide blend. *J. Appl. Polym. Sci.* **2012**, *126*, 1876–1884.
37 Zou, Z. M.; Sun, Z. Y.; An, L. J. Studies on droplet size distributions during coalescence in immiscible polymer blends filled with silica nanoparticles. *Chinese J. Polym. Sci.* **2014**, *32*, 255–267.
38 Anastasiadis, S. H.; Gancarz, I.; Koberstein, J. T. Compatibilizing effect of block copolymers added to the polymer/polymer interface. *Macromolecules* **1989**, *22*, 1449–1453.
39 Adedeji, A.; Lyu, S.; Macosko, C. W. Block copolymers in homopolymer blends: interface vs micelles. *Macromolecules* **2001**, *34*, 8663–8668.
40 Ginzburg, V. V. Influence of nanoparticles on miscibility of polymer blends. A simple theory. *Macromolecules* **2005**, *38*, 2362–2367.
41 Virgilio, N.; Favis, B. D. Self-assembly of Janus composite droplets at the interface in quaternary immiscible polymer blends. *Macromolecules* **2011**, *44*, 5850–5856.
42 Walther, A.; Matussek, K.; Müller, A. H. E. Engineering nanostructured polymer blends with controlled nanoparticle location using Janus particles. *ACS Nano* **2008**, *2*, 1167–1178.
43 Walther, A.; Müller, A. H. E. Janus particles: synthesis, self-assembly, physical properties, and applications. *Chem. Rev.* **2013**, *113*, 5194–5261.
44 Erhardt, R.; Böker, A.; Zettl, H.; Kaya, H.; Pyckhout-Hintzen, W.; Krausch, G.; Abetz V.; Müller, A. H. E. Janus micelles. *Macromolecules* **2001**, *34*, 1069–1075.
45 Bayer, U.; Stadler, R. Synthesis and properties of amphiphilic "dumbbell"-shaped grafted block copolymers, 1. Anionic synthesis *via* a polyfunctional initiator. *Macromol. Chem. Phys.* **1994**, *195*, 2709–2722.
46 Förster, S.; Antonietti, M. Amphiphilic block copolymers in structure-controlled nanomaterial hybrids. *Adv. Mater.* **1998**, *10*, 195–217.
47 Stewart, S.; Liu, G. Hollow nanospheres from polyisoprene-block-poly (2-cinnamoylethyl methacrylate)-block-poly(*tert*-butyl acrylate). *Chem. Mater.* **1999**, *11*, 1048–1054.
48 Bieringer, R.; Abetz, V.; Müller, A. H. E. Triblock copolyampholytes from 5-(*N*,*N*-dimethylamino) isoprene, styrene, and methacrylic acid: synthesis and solution properties. *Eur. Phys. J. E* **2001**, *5*, 5–12.
49 Sun, Y. J.; Liang, F. X.; Qu, X. Z.; Wang, Q.; Yang, Z. Z. Robust reactive Janus composite particles of snowman shape. *Macromolecules* **2015**, *48*, 2715–2722.
50 Yu, X. T.; Sun, Y. J.; Liang, F. X.; Jiang, B. Y.; Yang, Z. Z. Triblock Janus particles by seeded emulsion polymerization. *Macromolecules* **2019**, *52*, 96–102.
51 Liang, F. X.; Shen, K.; Qu, X. Z.; Zhang, C. L.; Wang, Q., Li, J. G.; Yang, Z. Z. Inorganic Janus nanosheets. *Angew. Chem. Int. Edit.* **2011**, *50*, 2379–2382.
52 Chen, Y.; Liang, F. X.; Yang, H. L.; Zhang, C. L.; Wang, Q.; Qu, X. Z.; Yang, Z. Z. Janus nanosheets of polymer-inorganic layered composites. *Macromolecules* **2012**, *45*, 1460–1467.
53 Liu, Y.; Abetz, V.; Müller, A. H. Janus cylinders. *Macromolecules* **2003**, *36*, 7894–7898.
54 Xia, Y.; Olsen, B. D.; Kornfield, J. A.; Grubbs, R. H. Efficient synthesis of narrowly dispersed brush copolymers and study of their assemblies: the importance of side chain arrangement. *J. Am. Chem. Soc.* **2009**, *131*, 18525–18532.
55 Zhao, X.; Wang, H.; Fu, Z.; Li, Y. Enhanced interfacial adhesion by reactive carbon nanotubes: new route to high-performance immiscible polymer blend nanocomposites with simultaneously enhanced toughness, tensile strength, and electrical conductivity. *ACS Appl. Mater. Interfaces* **2018**, *10*, 8411–8416.
56 Fu, Z.; Wang, H.; Zhao, X.; Li, X.; Gu, X.; Li, Y. Flame-retarding nanoparticles as the compatibilizers for immiscible polymer blends: simultaneously enhanced mechanical performance and flame retardancy. *J. Mater. Chem. A* **2019**, *7*, 4903–4912.
57 Li, X.; Fu, Z.; Gu, X.; Liu, H.; Wang, H.; Li, Y. Interfacially located nanoparticles: Barren nanorods versus polymer grafted nanorods. *Compos. Pt. B-Eng.* **2020**, *198*, 108153.
58 Bryson, K. C.; Löbling, T. I.; Müller, A. H. E.; Russell, T. P.; Hayward, R. C. Using Janus nanoparticles to trap polymer blend morphologies during solvent-evaporation-induced demixing. *Macromolecules* **2015**, *48*, 4220–4227.
59 Bahrami, R.; Löbling, T. I.; Gröschel, A. H.; Schmalz, H.; Müller, A. H. E.; Altstädt, V. The impact of Janus nanoparticles on the compatibilization of immiscible polymer blends under technologically relevant conditions. *ACS Nano* **2014**, *8*, 10048–10056.
60 Wang, H. T.; Fu, Z. A.; Zhao, X. W.; Li, Y. J.; Li, J. Y. Reactive nanoparticles compatibilized immiscible polymer blends: synthesis of reactive SiO_2 with long poly(methyl methacrylate) chains and the *in situ* formation of Janus SiO_2 nanoparticles anchored exclusively at the interface. *ACS Appl. Mater. Interfaces* **2017**, *9*, 14358–14370.
61 Wang, H.; Dong, W.; Li, Y. Compatibilization of immiscible polymer blends using in situ formed Janus nanomicelles by reactive blending. *ACS Macro Lett.* **2015**, *4*, 1398–1403.
62 Wang, H. T.; Fu, Z. A.; Dong, W. Y.; Li, Y. J.; Li, J. Y. Formation of interfacial Janus nanomicelles by reactive blending and their compatibilization effects on immiscible polymer blends. *J. Phys. Chem. B* **2016**, *120*, 9240–9252.
63 Fu, Z.; Wang, H.; Zhao, X.; Horiuchi, S.; Li, Y. Immiscible polymer blends compatibilized with reactive hybrid nanoparticles: Morphologies and properties. *Polymer* **2017**, *132*, 353–361.
64 Nie, H.; Zhang, C.; Liu, Y.; He, A. Synthesis of Janus rubber hybrid particles and interfacial behavior. *Macromolecules* **2016**, *49*, 2238–2244.
65 Xu, W.; Chen, J.; Chen, S.; Chen, Q.; Lin, J.; Liu, H. Study on the compatibilizing effect of Janus particles on liquid isoprene rubber/epoxy resin composite materials. *Ind. Eng. Chem. Res.* **2017**, *56*, 14060–14068.
66 Cheng, W.; Xu, Z.; Chen, S.; Ai, J.; Lin, J.; Lin, J.; Chen, Q. Compatibilization behavior of double spherical TETA–SiO_2@PDVB Janus particles anchored at the phase interface of acrylic resin/epoxy resin (AR/EP) polymer blends. *ACS omega* **2019**, *4*, 17607–17614.
67 Parpaite, T.; Otazaghine, B.; Caro, A. S.; Taguet, A.; Sonnier, R.; Lopez-Cuesta, J. M. Janus hybrid silica/polymer nanoparticles as effective compatibilizing agents for polystyrene/polyamide-6 melted blends. *Polymer* **2016**, *90*, 34–44.
68 Caro, A. S.; Parpaite, T.; Otazaghine, B.; Taguet, A.; Lopez-Cuesta, J. M. Viscoelastic properties of polystyrene/polyamide-6 blend

compatibilized with silica/polystyrene Janus hybrid nanoparticles. *J. Rheol.* **2017**, *61*, 305–310.
69 You, W.; Yu, W. Onset reduction and stabilization of cocontinuous morphology in immiscible polymer blends by snowmanlike Janus nanoparticles. *Langmuir* **2018**, *34*, 11092–11100.
70 He, H.; Liang, F. Engineering polymer blends with controllable interfacial location of Janus particles as compatibilizers. *Chem. Mater.* **2022**, *34*, 3806–3818.
71 Nie, H.; Liang, X.; He, A. Enthalpy-enhanced Janus nanosheets for trapping nonequilibrium morphology of immiscible polymer blends. *Macromolecules* **2018**, *51*, 2615–2620.
72 Han, X.; Liang, X.; Cai, L.; He, A.; Nie, H. Amphiphilic Janus nanosheets by grafting reactive rubber brushes for reinforced rubber materials. *Polym. Chem.* **2019**, *10*, 5184–5190.
73 Weiss, S.; Hirsemann, D.; Biersack, B.; Ziadeh, M.; Müller, A. H. E.; Breu, J. Hybrid Janus particles based on polymer-modified kaolinite. *Polymer* **2013**, *54*, 1388–1396.
74 Hu, L.; Han, Y.; Rong, C.; Wang, X.; Wang, H.; Li, Y. Interfacial engineering with rigid nanoplatelets in immiscible polymer blends: interface strengthening and interfacial curvature controlling. *ACS Appl. Mater. Interfaces* **2022**, *14*, 11016–11027.
75 Zhang, M.; Jiang, C.; Wu, Q.; Zhang, G.; Liang, F.; Yang, Z. Poly(lactic acid)/poly(butylene succinate) (PLA/PBS) layered composite gas barrier membranes by anisotropic Janus nanosheets compatibilizers. *ACS Macro Lett.* **2022**, *11*, 657–662.
76 Huang, M.; Li, Z.; Guo, H. The effect of Janus nanospheres on the phase separation of immiscible polymer blends via dissipative particle dynamics simulations. *Soft Matter* **2012**, *8*, 6834–6845.
77 Huang, M.; Guo, H. The intriguing ordering and compatibilizing performance of Janus nanoparticles with various shapes and different dividing surface designs in immiscible polymer blends. *Soft Matter* **2013**, *9*, 7356–7368.
78 Zhou, Y.; Huang, M.; Lu, T.; Guo, H. Nanorods with different surface properties in directing the compatibilization behavior and the morphological transition of immiscible polymer blends in both shear and shear-free conditions. *Macromolecules* **2018**, *51*, 3135–3148.
79 Zhou, C.; Luo, S. K.; Sun, Y.; Zhou, Y.; Qian, W. Dissipative particle dynamics studies on the interfacial tension of A/B homopolymer blends and the effect of Janus nanorods. *J. Appl. Polym. Sci.* **2016**, 133.
80 Estridge, C. E.; Jayaraman, A. Diblock copolymer grafted particles as compatibilizers for immiscible binary homopolymer blends. *ACS Macro Lett.* **2015**, *4*, 155–159.
81 Li, W.; Dong, B.; Yan, L. T. Janus nanorods in shearing-to-relaxing polymer blends. *Macromolecules* **2013**, *46*, 7465–7476.

https://doi.org/10.1007/s10118-022-2878-y